

NUMERICAL ANALYSIS AND SCIENTIFIC COMPUTING
PREPRINT SERIA

**Comparison of time discretization
schemes to simulate the motion of an
inextensible beam**

S. BASTING A. QUAINI R. GLOWINSKI S. ČANIĆ

PREPRINT #25



DEPARTMENT OF MATHEMATICS
UNIVERSITY OF HOUSTON

DECEMBER 2013

Comparison of time discretization schemes to simulate the motion of an inextensible beam

S. Basting¹, A. Quaini², R. Glowinski² and S. Canic²

¹ Friedrich-Alexander-University Erlangen-Nuremberg, Cauerstr. 11, 91058 Erlangen, Germany basting@math.fau.de

² University of Houston, 4800 Calhoun Rd, Houston TX 77204, USA
{[quaini](mailto:quaini@math.uh.edu),[roland](mailto:roland@math.uh.edu),[canic](mailto:canic@math.uh.edu)}@math.uh.edu

Abstract. We compare three different time discretization schemes in combination with an augmented Lagrangian method to simulate the motion of an inextensible beam. The resulting saddle-point problem is solved with an Uzawa-Douglas-Rachford algorithm. The three schemes are tested on a benchmark with an analytical solution and on a more challenging application. We found that in order to obtain optimal convergence behavior in time, the stopping tolerance for the Uzawa-type algorithm should be balanced against the time step size.

1 Introduction

The motion of an inextensible beam, while well studied (see, e.g. [4] and references therein), remains to be a challenging problem numerically. The main difficulties stem from the nonlinearity due to the inextensibility condition, and the choice of appropriate time discretization scheme that is stable and accurate (see [5] for a survey on different schemes). In this work, we evaluate the performance of the Houbolt scheme, a generalized Crank-Nicolson scheme, and a Newmark scheme, which are combined with an Uzawa-type algorithm for solving the saddle-point problem associated with an augmented Lagrangian method employed to handle the inextensibility condition.

2 Motion of an inextensible beam

We consider an inextensible elastic beam in static and dynamic regimes, assuming negligible torsional effects. We will denote by ρ the linear density (i.e. mass per unit length), by L the length, and by EI the flexural stiffness of the beam. We will use the following notation, with s denoting arc length and t time: $\mathbf{y}' = \frac{\partial \mathbf{y}}{\partial s}$, $\dot{\mathbf{y}} = \frac{\partial \mathbf{y}}{\partial t}$, $\mathbf{y}'' = \frac{\partial^2 \mathbf{y}}{\partial s^2}$, $\ddot{\mathbf{y}} = \frac{\partial^2 \mathbf{y}}{\partial t^2}$.

2.1 The static problem

We assume that the beam is subject to external forces \mathbf{f} and that the strain-stress relation is linear. The position of the beam at the equilibrium config-

uration is solution of a non-convex constrained problem:

$$\mathbf{x} = \arg \min_{\mathbf{y} \in K} J(\mathbf{y}), \text{ where } J(\mathbf{y}) = \frac{1}{2} \int_0^L EI |\mathbf{y}''|^2 ds - \int_0^L \mathbf{f} \cdot \mathbf{y} ds, \quad (1)$$

and $K = \{\mathbf{y} \in (H^2(0, L))^2, |\mathbf{y}'| = 1, \text{ plus boundary conditions}\}$.

To treat the inextensibility condition $|\mathbf{y}'| = 1$, which is a quadratic constraint, we use an augmented Lagrangian Method (see, e.g., [1–4]). Let us introduce the following space and set:

$$\begin{aligned} V &= \{\mathbf{y} \in (H^2(0, L))^2, \text{ plus boundary conditions}\}, \\ \mathcal{Q} &= \{\mathbf{q} \in (L^2(0, L))^2, |\mathbf{q}| = 1 \text{ a.e. on } (0, L)\}. \end{aligned}$$

The static problem (1) is equivalent to

$$\{\mathbf{x}, \mathbf{x}'\} = \arg \min_{\{\mathbf{y}, \mathbf{q}\} \in W} J(\mathbf{y}), \quad \text{with } W = \{\mathbf{y} \in V, \mathbf{q} \in \mathcal{Q}, \mathbf{y}' - \mathbf{q} = \mathbf{0}\}.$$

With $r > 0$, we introduce the following augmented Lagrangian functional:

$$\mathcal{L}_r(\mathbf{y}, \mathbf{q}; \boldsymbol{\mu}) = J(\mathbf{y}) + \frac{r}{2} \int_0^L |\mathbf{y}' - \mathbf{q}|^2 ds + \int_0^L \boldsymbol{\mu} \cdot (\mathbf{y}' - \mathbf{q}) ds \quad (2)$$

Let $\{\mathbf{x}, \mathbf{p}; \boldsymbol{\lambda}\}$ be a saddle point of \mathcal{L}_r over $(V \times \mathcal{Q}) \times (L^2(0, L))^2$. Then \mathbf{x} is a solution of the static problem (1) and $\mathbf{p} = \mathbf{x}'$. In order to solve the above saddle-point problem, we employ the algorithm called ALG2 in, e.g., [2,4]. As shown in, e.g., [2], this Uzawa-type algorithm is in fact a ‘disguised’ Douglas-Rachford operator-splitting scheme. It reads as follow:

Step 0: The initial guess $\{\mathbf{x}_{-1}, \boldsymbol{\lambda}_0\} \in V \times (L^2(0, L))^2$ is given.

Then, for $k \geq 0$, $\{\mathbf{x}_{k-1}, \boldsymbol{\lambda}_k\}$ being known, proceed with:

Step 1: Find $\mathbf{p}_k \in \mathcal{Q}$ such that:

$$\mathcal{L}_r(\mathbf{x}_{k-1}, \mathbf{p}_k; \boldsymbol{\lambda}_k) \leq \mathcal{L}_r(\mathbf{x}_{k-1}, \mathbf{q}; \boldsymbol{\lambda}_k), \quad \forall \mathbf{q} \in \mathcal{Q}.$$

Step 2: Find $\mathbf{x}_k \in V$ such that:

$$\mathcal{L}_r(\mathbf{x}_k, \mathbf{p}_k; \boldsymbol{\lambda}_k) \leq \mathcal{L}_r(\mathbf{y}, \mathbf{p}_k; \boldsymbol{\lambda}_k), \quad \forall \mathbf{y} \in V. \quad (3)$$

Step 3: Update the Lagrange multipliers by:

$$\boldsymbol{\lambda}_{k+1} = \boldsymbol{\lambda}_k + r((\mathbf{x}_k)' - \mathbf{p}_k).$$

If the boundary conditions for problem (1) are $\mathbf{y}(0) = \mathbf{x}_A$ and $\mathbf{y}'(0) = \mathbf{x}_B$, then the test function space at step 2 is defined by:

$$V_0 = \{\mathbf{y} \in (H^2(0, L))^2, \mathbf{y}(0) = \mathbf{0}, \mathbf{y}'(0) = \mathbf{0}\}.$$

To obtain \mathbf{p}_k at step 1, we have to solve the minimization problem:

$$\min_{|\mathbf{q}|=1} \mathcal{L}_r(\mathbf{x}_{k-1}, \mathbf{q}; \boldsymbol{\lambda}_k), \text{ with the solution } \mathbf{p}_k = \frac{r(\mathbf{x}_{k-1})' + \boldsymbol{\lambda}_k}{|r(\mathbf{x}_{k-1})' + \boldsymbol{\lambda}_k|}. \quad (4)$$

Problem (3) can be stated as the equivalent problem: Find $\mathbf{x}_k \in V$ such that for all $\mathbf{y} \in V_0$:

$$\int_0^L EI \mathbf{x}_k'' \cdot \mathbf{y}'' ds + r \int_0^L \mathbf{x}_k' \cdot \mathbf{y}' ds = \int_0^L \mathbf{f} \cdot \mathbf{y} ds + \int_0^L (r\mathbf{p}_k - \boldsymbol{\lambda}_k) \cdot \mathbf{y}' ds.$$

Step 1, 2, and 3 are repeated till the following stopping criterion is satisfied:

$$\frac{\|\mathbf{x}_{k+1} - \mathbf{x}_k\|}{\|\mathbf{x}_k\|} < \epsilon. \quad (5)$$

2.2 The dynamic problem

Using the virtual work principle, the beam motion for $t \in [0, T]$ is modeled by: Find $\mathbf{x}(t) \in K_t$:

$$\int_0^L \rho \ddot{\mathbf{x}} \cdot \mathbf{y} ds + \int_0^L EI \mathbf{x}'' \cdot \mathbf{y}'' ds = \int_0^L \mathbf{f} \cdot \mathbf{y} ds, \quad \forall \mathbf{y} \in dK_t(\mathbf{x}), \quad (6)$$

with

$$K_t = \{\mathbf{y} \in (H^2(0, L))^2, |\mathbf{y}'| = 1, \mathbf{y}(0) = \mathbf{x}_A(t), \mathbf{y}'(0) = \mathbf{x}_B(t)\}, \quad (7)$$

$$dK_t(\mathbf{x}) = \{\mathbf{y} \in (H^2(0, L))^2, \mathbf{x}' \cdot \mathbf{y}' = 0, \mathbf{y}(0) = \mathbf{0}, \mathbf{y}'(0) = \mathbf{0}\}, \quad (8)$$

and initial conditions $\mathbf{x}(s, 0) = \mathbf{x}_0(s)$ and $\dot{\mathbf{x}}(s, 0) = \mathbf{x}_1(s)$. Weak formulation (6) assumes that at $s = L$ natural boundary conditions $\mathbf{x}''(L) = 0$ and $\mathbf{x}'''(L) = 0$ are imposed. Note that problem (6) in strong form reads: $\rho \ddot{\mathbf{x}} + EI \mathbf{x}'''' = \mathbf{f}$.

For the time discretization of problem (6) we will consider three schemes: a generalized Crank-Nicolson scheme, the Houbolt scheme, and a Newmark scheme (see, e.g., [4]). All these schemes are known to be second order accurate for linear problems. Let Δt be a time discretization step and set $t^n = n\Delta t$, for $n = 1, \dots, N$, with $N = T/\Delta t$. The time discrete problem reads: Find $\mathbf{x}^{n+1} \in K_{t^{n+1}}$:

$$\int_0^L \rho \ddot{\mathbf{x}}^{n+1} \cdot \mathbf{y} ds + \int_0^L EI \tilde{\mathbf{x}}'' \cdot \mathbf{y}'' ds = \int_0^L \tilde{\mathbf{f}} \cdot \mathbf{y} ds, \quad (9)$$

Table 1: Definition of $\ddot{\mathbf{x}}^{n+1}$, $\tilde{\mathbf{x}}$, and $\tilde{\mathbf{f}}$ in (9) for the time discretization schemes under consideration: Generalized Crank-Nicolson (GCN), Houbolt, and Newmark with $\beta = 1/4$, $\gamma = 1/2$. For GCN, $0 < \alpha < 1/2$.

	GCN	Houbolt	Newmark*
$\ddot{\mathbf{x}}^{n+1}$	$\frac{\mathbf{x}^{n+1} - 2\mathbf{x}^n + \mathbf{x}^{n-1}}{\Delta t^2}$	$\frac{2\mathbf{x}^{n+1} - 5\mathbf{x}^n + 4\mathbf{x}^{n-1} - \mathbf{x}^{n-2}}{\Delta t^2}$	$\frac{\mathbf{v}^{n+1} - \mathbf{v}^n}{\Delta t}$
$\tilde{\mathbf{x}}$	$\alpha\mathbf{x}^{n+1} + (1 - 2\alpha)\mathbf{x}^n + \alpha\mathbf{x}^{n-1}$	\mathbf{x}^{n+1}	$\frac{\mathbf{x}^{n+1} + \mathbf{x}^n}{2}$
$\tilde{\mathbf{f}}$	$\alpha\mathbf{f}^{n+1} + (1 - 2\alpha)\mathbf{f}^n + \alpha\mathbf{f}^{n-1}$	\mathbf{f}^{n+1}	$\frac{\mathbf{f}^{n+1} + \mathbf{f}^n}{2}$
* with $\frac{\mathbf{v}^{n+1} + \mathbf{v}^n}{2} = \frac{\mathbf{x}^{n+1} - \mathbf{x}^n}{\Delta t}$.			

for all $\mathbf{y} \in dK_{t^{n+1}}(\mathbf{x}^{n+1})$. The definition of $\ddot{\mathbf{x}}^{n+1}$, $\tilde{\mathbf{x}}$, and $\tilde{\mathbf{f}}$ in (9) is reported in table 1 for each scheme under consideration. Time discretization approximates problem (6) by a sequence of quasi-static problems for which ALG2 still applies. For the space discretization of problem (9) we use a third order Hermite finite element method (see, e.g., [1]). For details about the discretization of $\mathbf{p}_k \in \mathcal{Q}$ (4) and $\boldsymbol{\lambda}_k \in (L^2(0, L))^2$ we refer to [4].

3 Numerical results

3.1 Benchmark with analytical solution

We consider $s \in [0, \pi/2]$ and $t \in [0, 1]$, and a family of exact solutions which is given by:

$$\mathbf{x}_{ex}(s, t) = (\phi(t))^{-1} [\cos(s\phi(t)), \sin(s\phi(t))]^T. \quad (10)$$

Notice that solution (10) satisfies the inextensibility condition $|\mathbf{x}'| = 1$ point-wise for every function $\phi(t)$. We chose $\phi(t) = e^t$, for which the solution is a quarter of a circle of initial radius 1 that coils over time as its radius decreases (see Fig. 1). At $s = 0$ and $s = \pi/2$, we impose the values of \mathbf{x} and \mathbf{x}' . The forcing term \mathbf{f}_{ex} needed to recover solution (10) is found by plugging \mathbf{x}_{ex} into the governing differential equations (strong form):

$$\rho\ddot{\mathbf{x}}_{ex} + EI\mathbf{x}_{ex}'''' = \mathbf{f}_{ex}. \quad (11)$$

For simplicity, we set $\rho = 1 \text{ Kg/m}^3$ and $EI = 1 \text{ Kg m}^3/\text{s}^2$. The forcing term \mathbf{f}_{ex} is made up of two contributions: an external body force \mathbf{f}_b and an internal force due to inextensibility \mathbf{f}_{in} . To find \mathbf{f}_{in} , we notice that problem

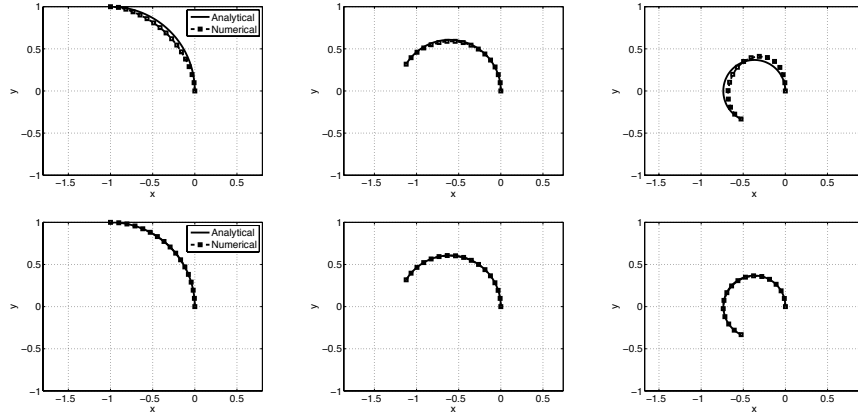


Fig. 1: Comparison between analytical and numerical solution at $t = 0$ s (left), $t = 0.5$ s (center), $t = 1$ s (right) for two values of stopping tolerance: $\epsilon = 10^{-1}$ (top) and $\epsilon = 10^{-5}$ (bottom). The legend in the subfigures on the left is common to all the subfigures.

(6) is equivalent to minimization problem $\mathbf{x} = \arg \min_{\mathbf{y} \in K_t} J(\mathbf{y})$, where the total energy of the beam can be written as:

$$J(\mathbf{y}) = \frac{1}{2} \int_0^L \rho |\dot{\mathbf{y}}|^2 ds + \frac{1}{2} \int_0^L EI |\mathbf{y}''|^2 ds + \int_0^L \lambda (|\mathbf{y}'|^2 - 1) ds - \int_0^L \mathbf{f} \cdot \mathbf{y} ds,$$

and λ is a scalar function that depends on time only. If the above functional attains its minimum at \mathbf{x} , it follows that its Gâteaux derivative must be vanishing at \mathbf{x} , leading to

$$\int_0^L \rho \ddot{\mathbf{x}} \cdot \mathbf{y} ds + \int_0^L EI \mathbf{x}'' \cdot \mathbf{y}'' ds = \int_0^L \mathbf{f} \cdot \mathbf{y} ds + \int_0^L (\lambda \mathbf{x}')' \cdot \mathbf{y} ds,$$

for all $\mathbf{y} \in dK_t(\mathbf{x})$. The second integral on the right-hand side (equal to zero if $\mathbf{y} \in dK_t(\mathbf{x})$, which is not the case for the test functions used in the computations) gives the explicit contribution of \mathbf{f}_{in} . We are going to check the convergence rates in time for the three schemes in table 1 in two cases:

- linear case: when the forcing term is \mathbf{f}_{ex} the inextensibility condition becomes inactive due to the fact that \mathbf{f}_{ex} is given by (11) and the problem reduces to the linear beam equation;
- nonlinear case: when then forcing term is $\mathbf{f}_{ex} + (\lambda \mathbf{x}')'$, with, e.g., $\lambda = 1$, the problem becomes nonlinear and the inextensibility is treated via the augmented Lagrangian method described in Sec. 2.

The space resolution Δs is taken to be $\pi/240$. For the generalized Crank-Nicolson scheme, we set $\alpha = 1/4$ since in linear cases this choice leads to

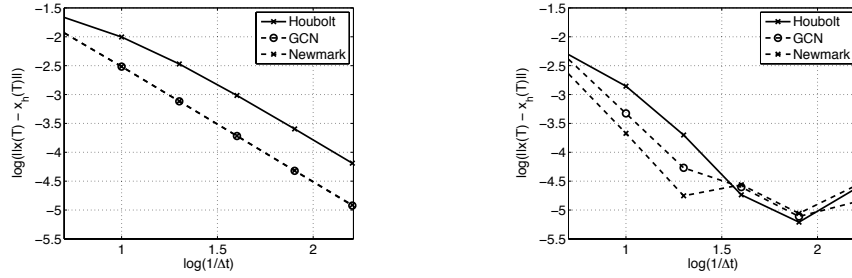
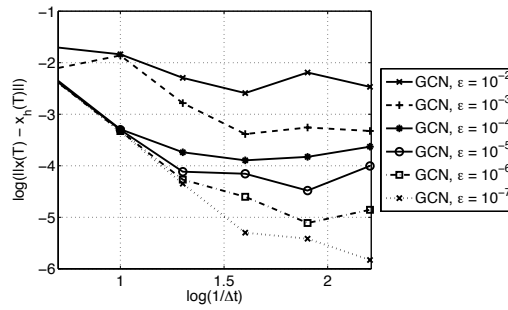


Fig. 2: Convergence rate in time for the generalized Crank-Nicolson (GCN) scheme, the Houbolt scheme, and the Newmark scheme in the linear (left) and nonlinear/inextensible (right) case.

Fig. 4: Convergence rate in time for the generalized Crank-Nicolson (GCN) scheme in the nonlinear case for different values of the stopping tolerance ϵ .



an unconditionally stable scheme which possesses a very small numerical dissipation compared, e.g., to Houbolt method [1]. In the nonlinear case, for ALG2 we set stopping tolerance $\epsilon = 10^{-5}$ (5) and $r = 10^2$. In Fig. 2, we plot the L^2 norm of the difference between the exact solution \mathbf{x}_{ex} and the numerical solution \mathbf{x}_h at $t = 1$ against time step ($\Delta t = 0.2, 0.1, 0.05, 0.025, 0.0125, 0.00625$) for the linear and nonlinear cases. The rates predicted by the theory are achieved in the linear case: all the schemes are of second order. We remark that for a given value of Δt the Houbolt scheme is less accurate than the other two. In the nonlinear case, for all the schemes the order of convergence is even larger than 2 provided that Δt is less than a critical value for which the error reaches the stopping tolerance ϵ . If Δt is greater than that critical value, the error remains unchanged or even slightly increases.

As noted earlier, the error depends on the choice of ϵ . To illustrate this, in Fig. 1 we compare analytical solution (10) with the numerical solution at $t = 0, 0.5, 1$ s and for two values of the stopping tolerance: $\epsilon = 10^{-1}$ (top) and $\epsilon = 10^{-5}$ (bottom), every other discretization parameter being the same. For $\epsilon = 10^{-1}$ the difference between analytical and numerical solution is clearly visible, while for $\epsilon = 10^{-5}$ the two solutions are almost superimposed.

Finally, in order to evaluate the dependence of the error on ϵ , we report in Fig. 4 the convergence rates in time for the generalized Crank-Nicolson scheme in the nonlinear case for different values of the stopping tolerance $\epsilon = 10^{-2}, 10^{-3}, 10^{-4}, 10^{-5}, 10^{-6}, 10^{-7}$. The values for Δt and Δs are the same as those used for the results in Fig. 2. We see that at the critical value of Δt the curves reach a plateau for all the values of ϵ , indicating that for a given value of ϵ it does not make sense to choose a time step size that is too small. Our computations seem to indicate that Δt should be larger than $\sqrt{\epsilon}$.

3.2 Swinging beam

The second test problem we consider involves the two-dimensional motion of a beam subject to gravity, which is an established test problem [3]. The beam is attached at one extremity (denoted by A here) and free at the other one (B). We aim at comparing our results with those reported in [3]. We have: $L = 32.6$ m, $EI = 700$ Kg m³/s², $\rho = 7.67$ Kg/m. At $A = (0, 0)$ the beam is fixed and $B|_{t=0} = (20, 0)$. The initial position is given by the solution of the static problem (1), with boundary conditions $\mathbf{x}(0) = (0, 0)$ and $\mathbf{x}(L) = (20, 0)$. The motion of the beam for $t \in [0, 10]$ s is visualized in

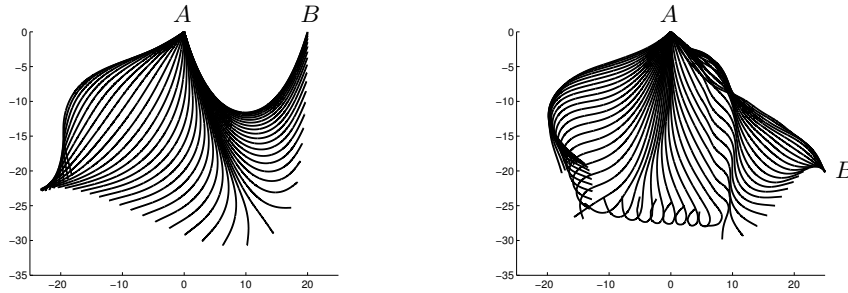


Fig. 5: Position of the beam every 0.1 s for $t \in [0, 5]$ s (left) and $t \in [5, 10]$ (right).

Fig. 5. For the results in Fig. 5, we have used the generalized Crank-Nicolson scheme ($\alpha = 1/4$) with $\Delta t = 0.01$, and $\Delta s = 32.6/60$. For ALG2, we have set $r = 10^5$ and $\epsilon = 10^{-5}$. Fig. 5 is qualitatively very similar to the corresponding pictures in reference [3].

Next, we compare the displacement over time of the beam tip given by the generalized Crank-Nicolson scheme, the Houbolt scheme, and the Newmark scheme (see table 1). The ALG2 and discretization parameters are the same used for the results in Fig. 5. Fig. 6 shows the x and y components of the displacement for the three methods. We see that all the schemes are in good agreement, with the Houbolt scheme giving larger oscillations than the other two schemes.

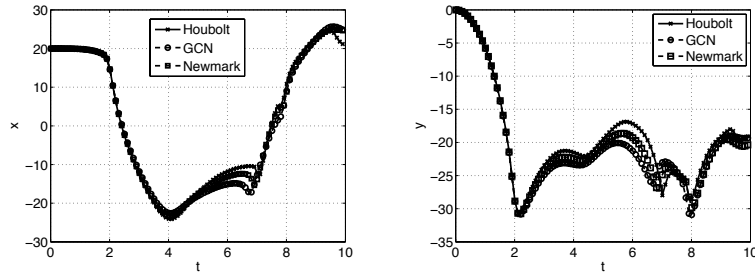


Fig. 6: Displacement of the beam tip for $t \in [0, 10]$: x -component (left) and y -component (right).

4 Conclusions

We compared three different time discretization schemes (the Houbolt scheme, a generalized Crank-Nicolson scheme, and a Newmark scheme) in combination with an augmented Lagrangian method to simulate the motion of an inextensible beam. While all these schemes are known to be second order accurate in time for linear problems, for the nonlinear problem considered here, our numerical simulations for a benchmark problem with analytical solution indicate that the accuracy increases when they are combined with an Uzawa-type algorithm to account for inextensibility. Special care has to be taken in selecting the termination criterion. Our computations suggest that the stopping tolerance for the Uzawa-type algorithm should be balanced against the time step size in a rather restrictive manner.

References

1. J.-F. BOURGAT, M. DUMAY, AND R. GLOWINSKI, *Large displacement calculations of inextensible pipelines by finite element and nonlinear programming methods*, SIAM J. Sci. Stat. Comput. **1** (1980), 34–81.
2. M. FORTIN AND R. GLOWINSKI, *Augmented Lagrangian methods: Application to the numerical solution of boundary value problem*, North-Holland, Amsterdam, 1983.
3. R. GLOWINSKI AND M. HOLMSTROM, *Constrained motion problems with applications by nonlinear programming methods*, Surv. Math. Ind. **5** (1995), 75–108.
4. R. GLOWINSKI AND P. L. TALLEC, *Augmented Lagrangian and operator-splitting methods in nonlinear mechanics*, SIAM, Philadelphia, 1988.
5. K. SUBBARAJ AND M. DOKAINISH, *A survey of direct time-integration methods in computational structural dynamics II. Implicit methods*, Computers & Structures **32**:6 (1989), 1387 – 1401.